JOURNAL OF MECHANICAL ENGINEERING AND SCIENCES
ISSN: 2289-4659 e-ISSN: 2231-8380
VOLUME 17, ISSUE 2, 2023, 9507 – 9519
DOI: https://doi.org/10.15282/jmes.17.2.2023.9.0753

RESEARCH ARTICLE

A numerical investigation of effects of chemical kinetic mechanisms on the structure of turbulent jet diffusion H_2/air flame with Lagrangian PDF method

M. Senouci[1]*, A. Bounif[2], H. Merouane[3] and M. Boukhelef[3]

[1] Laboratoire des Systèmes Complexes, Higher School of Electrical and Energetic Engineering of Oran, Chemin Vicinal N9 Oran 31000, Algeria
Phone: +213041240937; Fax: +213041627113
[2] Faculty of Science and Technology, University Belhadj Bouchaib of Ain Temouchent, Bp 284 Sidi bel Abbes 46000 Ain Temouchent, Algeria
[3] Faculty of Science and Technology, University Mustapha Stambouli of Mascara, Bp 305 Route de Mamounia Mascara, Algeria

ABSTRACT - Many physical phenomena characteristic of reactive flows are controlled by the detail of the chemical kinetics of combustion. These include, for example, the ignition and extinction of a flame and the formation of polluting species. These phenomena require the use of detailed kinetic schemes including hundreds of species and thousands of reactions.The main objective of this work is to highlight the influence of chemical kinetics on the structure of turbulent jet diffusion H_2/air flame. Five improved hydrogen kinetic mechanisms have been tested in order to validate, compare and evaluate their effect on the scalar and dynamic fields of such flames. The effect of number particles used in Lagrangian PDF method on the temperature evoltution is also studied. A hybrid method, PDF Lagrangian coupled to the RSM turbulence model, is used in this work, for the numerical simulation. The micro-mixing term of the TPDF is modeled by the EMST model. This model, which describes well the physical process of mixing, has shown its capabilities to give good numerical results. The impact of these mechanisms on the numerical results of scalar and dynamic fields was discussed and compared with the experimental data. The scalar field is well influenced by the choice of the chemical kinetic mechanism. This is not the case of the dynamic field. A good agreement with experience is observed for detailed kinetic mechanisms. However, it has been noticed that simple and reduced mechanisms give also satisfactory results, particularly the reduced kinetic mechanism R12 wich includes 12 reaction and can be considered as a compromise among the five kinetic mechanisms. These mechanisms allows for a significant reduction in CPU time and storage memory. It was also observed that, for the two chemical kinetic mechanisms R12 and R27, the number of particles only affects the radial evolution.

ARTICLE HISTORY
Received : 17th Feb. 2023
Revised : 01st May 2023
Accepted : 18th May 2023
Published : 28th June 2023

KEYWORDS
PDF method
Turbulent diffusion flame
Chemical kinetics
Reacting flows
RMS model

1.0 INTRODUCTION

Today combustion remains one of the main means of energy conversion. In all practical cases of flow, the Reynolds numbers are large enough so that this combustion is in fact turbulent. The study of turbulent combustion is therefore of great interest, both on a fundamental and industrial level. Various methods are used in turbulent combustion modelling. One of the most commonly is the transported probability density function (TPDF) method [1, 2]. This method represents a very general statistical description of turbulent reactive flows. The Monte Carlo method is often used to solve the modeled PDF equation. The joint PDFs contain the most detailed information about the distribution of properties at a given position and time. In TPDF methods, the chemical source appears in closed form, which therefore allows the exact treatment of detailed combustion chemistry. Only, the molecular mixing term requires modelling. The molecular mixing term is modeled, here, by Euclidean minimum spanning tree (EMST) model. The EMST model, which provides a better description of the physical mixing process, is usually considered to be superior [3, 4]. The in-situ adaptive tabulation (ISAT) method is adopted to calculate the reaction source term [3, 5].

Studies on turbulent non-premixed hydrogen flames concentrate much more on the modelling of combustion and turbulence in hydrogen mixtures *(*H_2–N_2, H_2–He*)* and in the cases of pure hydrogen. The most used turbulence models in the calculation of such flames are the (k-ε) and the Reynolds stress models (RSM). The RSM model is highly recommended in the case of complex flows, particularly in the presence of strong anisotropy. This model, which gives a better prediction of complex flows, is used in this study. Many physical phenomena characteristic of reactive flows is controlled by the detail of the chemical kinetics of combustion. These include, for example, the ignition and extinction of a flame, the formation of polluting species. These phenomena require the use of detailed kinetic schemes including hundreds of species and thousands of reactions. The study of the effect of chemical kinetics on the quantitative and qualitative evolution of the scalar and dynamic fields of such flame using simple and reduced chemical kinetic mechanisms is very important. This will reveal the capacity of these schemes to improve the prediction of the evolution of the scalar and dynamic fields of these flames.

***CORRESPONDING AUTHOR | M. Senouci** | ✉ med_snci@yahoo.fr

Cao and Pope [6] studied the effect of kinetic mechanisms on PDF calculations of non-premixed piloted jet flames. Seven distinct kinetic mechanisms for methane are employed in PDF model calculations of the Barlow and Frank flames D, E and F in order to examine their capacity to represent the local extinction, reignition, and other chemical phenomena observed in this type of flames. A revised H_2/O_2 kinetic mechanism, which consists of 19 reversible elementary reactions, was validated by Juan Li [7] in his study on the hydrogen combustion. Excellent agreement of the model predictions with the experimental results has been observed. In the CFD simulations of Victor P. Zhukov [8], eight different kinetic models of hydrogen oxidation were tested and validated. The simulation of the ignition of hydrogen-air mixture revealed that the results are sensitive to the choice of kinetic model. The subsequent validation also showed that the detailed kinetic schemes are more accurate than the reduced ones but require significant CPU time and storage memory.

Five improved chemical kinetic mechanisms for hydrogen are tested in Lagrangian PDF method in order to compare and evaluate their effects on the scalar and dynamic fields of the turbulent jet diffusion H_2/air flame. The first (R7) is a simple mechanism containing seven steps reactions in which only four are reversible and is used by D. Fernández-Galisteo [9]. This mechanism gives good predictions of hydrogen-air lean-flame burning velocities. The second (R12) given by P. Boivin [10], consists of 12 steps reactions of which only six are reversible. It has been found that the twelve elementary reactions suffice to describe premixed and non-premixed flames, autoignition and detonations under conditions of practical interest. The third reduced mechanism (R16) consists of 16 reversible steps reactions and is used by X. Zhou [11]. The fourth detailed mechanism (R23), given by Wu [12], contains twenty three step reactions and has been used in our preceding work [3]. Finally, the fifth mechanism (R27), which is also a detailed mechanism, contains twenty seven irreversible step reactions and is given by E. Gutheil [13]. Also, two chemical kinetic mechanisms are chosen, those which gave good results, to study the impact of number particles used in Lagrangian PDF method.

In this work, the Lagrangian PDF methods is used to study the performance of five different chemical kinetic mechanisms of hydrogen in the calculation of turbulence-chemistry interactions in diffusion turbulent hydrogen/air flames. To our knowledge, few studies has been done on the effects of chemical kinetic mechanisms and the inlet jet velocity on the structure of scalar and dynamic fields of turbulent jet diffusion H_2/Air flame with PDF methods.

2.0 FAVRE AVERAGED GOVERNING EQUATIONS

The basic equations governing reactive turbulent flow are the equations of mass conservation, momentum conservation, and scalar conservation. These averaged equations are:

$$\frac{\partial \bar{\rho}}{\partial t} + \frac{\partial \bar{\rho}\tilde{u}_i}{\partial x_i} = 0 \tag{1}$$

$$\frac{\partial \bar{\rho}\tilde{u}_i}{\partial t} + \frac{\partial \bar{\rho}\,\tilde{u}_i\tilde{u}_j}{\partial x_j} = -\frac{\partial \bar{p}}{\partial x_i} + \frac{\partial \tilde{\tau}_{ij}}{\partial x_j} + \frac{\partial}{\partial x_j}\left(-\bar{\rho}\,\widetilde{u_i''u_j''}\right) \tag{2}$$

$$\frac{\partial \bar{\rho}\tilde{\phi}}{\partial t} + \frac{\partial \bar{\rho}\tilde{u}_i\tilde{\phi}}{\partial x_i} = -\frac{\partial J_i^{\phi}}{\partial x_i} - \frac{\partial}{\partial x_i}\left(-\bar{\rho}\,\widetilde{u_i''\phi''}\right) - \bar{\rho}\,\tilde{S}_{\phi} \tag{3}$$

The terms $\tilde{\tau}_{ij}$, $\bar{\rho}\,\widetilde{u_i''u_j''}$, $\bar{\rho}\,\widetilde{u_i''\phi''}$, J_i^{ϕ} and $\tilde{S}_{\phi}$ represent respectively the viscous stress, the Reynolds stress, the turbulent scalar flux, the molecular scalar flux and the source term. In highly turbulent flows, the molecular effects are weak compared to the turbulent agitation effects. To the conservation Eqs. (1) to (3), an additional equation defining the thermodynamic state of gas mixture is needed. It is given by:

$$P = \rho R T \sum_{\alpha=1}^{n} \frac{Y_{\alpha}}{W_{\alpha}} \tag{4}$$

3.0 MODELLING THE TURBULENCE

The nonlinearity of the governing equations makes it necessary to model unclosed terms occurring in the averaged equations. For the correlation of the fluctuations of the velocity, the RSM turbulence model is used. For the fluctuations of the scalar and velocity a gradient model is applied. The Reynolds stress equations are:

$$\frac{\partial}{\partial t}(\bar{\rho}\,\widetilde{u_i u_j}) + \frac{\partial}{\partial x_k}(\bar{\rho}\,\tilde{u}_k\,\widetilde{u_i u_j}) = \tilde{D}_{ij} + \tilde{P}_{ij} + \tilde{\phi}_{ij} - \frac{2}{3}\delta_{ij}\,\bar{\rho}\tilde{\varepsilon} \tag{5}$$

$$\frac{\partial}{\partial t}(\bar{\rho}\tilde{\varepsilon}) + \frac{\partial}{\partial x_k}(\bar{\rho}\,\tilde{u}_k\,\tilde{\varepsilon}) = \tilde{D}_{\varepsilon} + \bar{\rho}\frac{\tilde{\varepsilon}^2}{\tilde{k}}\tilde{\psi}(\varepsilon) \tag{6}$$

Detailed modelling of the various terms of Eqs. (5) and (6) is detailed in our previous work [3, 14]. The turbulent flux of the scalar is modelled as:

$$\overline{\rho}\,\widetilde{u_i''\phi''} = \frac{\mu_t}{\sigma_\phi}\frac{\partial \widetilde{\phi}}{\partial x_i} \tag{7}$$

where, μ_t is the turbulent viscosity and σ_ϕ is the effective Prandtl or Schmidt number for the scalar ϕ.

3.1 Combustion Modelling

Several models are employed to model turbulent diffusion flame. The most commonly used is the joint probability density function (JPDF) method. The JPDF is a function of time, spatial location and composition space. The determination of this JPDF allows the exact evaluation of the mean value for any function of these scalars.

In the present work, the joint PDF of composition vector is used [1, 3]. The transport equation of the joint composition mass density function $F_\phi(\Psi)$ of composition variables ϕ with sample space variables ψ is [1]:

$$\frac{\partial F_\phi}{\partial t} + \frac{\partial\, \widetilde{u}_i F_\phi}{\partial x_i} + \frac{\partial}{\partial \psi_\alpha}(S_\alpha(\psi) F_\phi) = -\frac{\partial}{\partial x_i}[<u_i''/\psi> F_\phi] - + \frac{\partial}{\partial \psi_\alpha}[\frac{1}{\rho(\psi)} < \frac{\partial J_i^\alpha}{\partial x_i} / \psi > F_\phi] \tag{8}$$

where, S_α is the composition source term and J_i^α represents the effect of micromixing. The three terms on the left-hand side appears in closed form; in particular the reaction source term S_α, which is the primary advantage of PDF method. The terms on the right-hand side must be modelled. Turbulent scalar flux is generally modeled by gradient transport assumption:

$$[<u_i''/\psi> F_\phi] = -\mu_t \frac{\partial [F_\phi / \overline{\rho}]}{\partial x_i} \tag{9}$$

The numerical conditions are shown in Table 1.

Table 1. Numerical conditions

Parameter	Details
Domain	2D axisymmetric
Solver	Steady, pressure based
Turbulence model	RSM model
Discretization scheme	PLDS
Mixing model	EMST model
ISAT error tolerance	10^{-4}
Particles numbers per computational cell	20

4.0 RESOLUTION METHOD

Eq. (8) is solved by hybrid Finite-Volume/Monte Carlo method presented in [15]. In this method, the finite volume method is used to solves the mean field equations of $\widetilde{u}$, $\widetilde{k}$, $\widetilde{\varepsilon}$ and $\overline{p}$. These values and the turbulent time scale $t = \widetilde{k}/\widetilde{\varepsilon}$ are then passed to the Monte Carlo method. In the Monte Carlo method, the particles move randomly through physical space by a spatially second order accurate Lagrangian method. The evolution of particles is due to different processes: convection, diffusion, mixing and reaction. These processes are treated in fractional steps as described in [3].

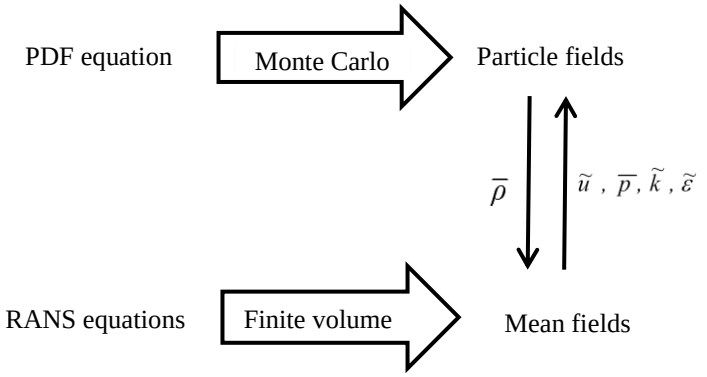

Figure 1. Hybrid solution method

5.0 GEOMETRIC CONFIGURATION AND BOUNDARY CONDITIONS

For calculations of reactive flows with axisymmetric geometry, a cylindrical coordinate system with the origin at the center of the fuel jet is used as shown in Figure 1. The computational domain covers a rectangular area of (50×*Dj*) in radial direction and (300×D_j) in axial direction. An orthogonal type of mesh was used. The mesh contains (200×156) nodes in the axial and radial direction respectively.

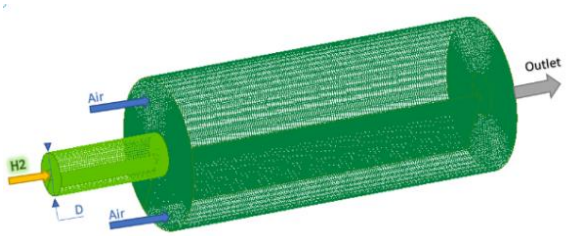

Figure 2. Simple diffusion flame configurations

Data at the inlet boundary are listed in Table 2.

Table 2. The inlet boundary data

Parameter	Details
Domaine	2D axisymmetric
Inlet diameter	Dj = 4 (mm)
Mean inlet velocity	Uj = 296 (m/s)
Coflow velocity	Uc = 1 (m/s)
Reynolds number	11544
Turbulent kinetic energy	$k = \frac{3}{2} I^2 u^2$ (m^2/s^2)[16]
Turbulent dissipation rate	$\varepsilon = \frac{C_\mu^{3/4} k^{3/2}}{L_m}$ (m^2/s^3)
Turbulent intensity	I ≈ 0.05
Mixing length	L_m = 0.07 R_j(m)
Inlet temperature	T_j = 300 (K)

Simplifying assumptions are presented in the Table 3.

Table 3. Simplifying assumptions

Parameter	Value
Mach numbers	Ma ≤ 0.3
Lewis numbers	Le = 1
Heat capacity at constant pressure of mixture	mixing law
radiation effect	negligible
Buoyancy effect	negligible

6.0 RESULTS AND DISCUSSION

In this section, the numerical results for mean mixture fraction, mean temperature and major chemical species are presented and compared with the experimental data of Barlow [17]. The impact of chemical kinetic mechanisms on dynamic field is also presented. In the computations, the spatial variables *r* and *x* are normalized respectively by the jet radius R_j (for radial evolution) and visible flame length L_{vis} (for axial evolution).

6.1 Effect of Chemical Kinetic Mechanisms

The effects of the chemical kinetic mechanisms on the axial evolution of the mean temperature are shown in Figure 3. The four kinetic mechanisms R12, R16, R23 and R27, which give practically the same maximum temperature, overpredict slightly the maximum experimental value of the temperature. This maximum value is in axial position the same. This is not the case for R7, which gives practically the same experimental maximum value of the temperature and its same axial position. Generally, qualitative agreements between the predictions and experimental data are observed for all kinetic mechanisms employed.

The impact of the chemical kinetic mechanisms on the radial profiles of the mean temperature at the three axial locations x/L_{vis}=1/8, 1/2 and 3/4 is shows in Figure 4(a), 4(b) and 4(c). In the region close to the nozzle exit (x/L_{vis}=1/8), Figure 4(a), a quantitative comparison shows that the peak temperature is well predicted by the two detailed kinetic mechanisms R23 and R27 and the reduced kinetic mechanisms R12. It can clearly see that this value of the maximum is practically the same for all three mechanisms and that the difference between the numerical results and the experiment is negligible. In addition, the R27 predicts best the radial position of the peak temperature. In the vicinity of the symmetry axis ($r/R_j \leq 2$), it is the two kinetic mechanisms R7 and R16 that predict well the experimental data. The most important remark concerns the reduced kinetic mechanisms R12. On the one hand, R12 predicts well the maximum temperature compared to R7 and R16. On the other hand, it gives good numerical results, in the regions very close to the symmetry axis, compared to R23 and R27. The reduced kinetic mechanisms R12 can be considered as a compromise between the four kinetic mechanisms. At large axial distances, the radial evolution of the temperature becomes insensitive to the choice of the chemical kinetic mechanisms. There is also very good agreement with experience in these regions.

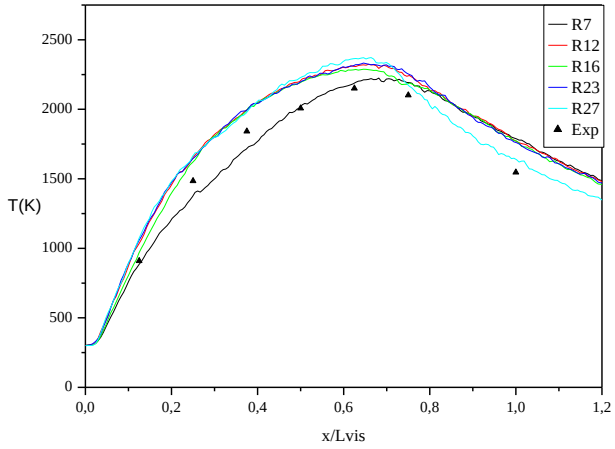

Figure 3. Centerline evolution of the temperature

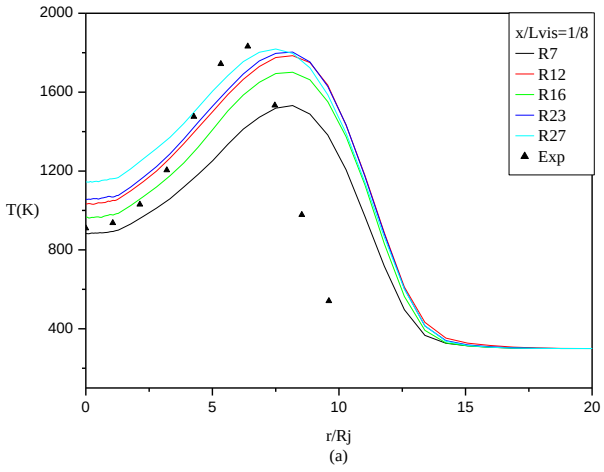

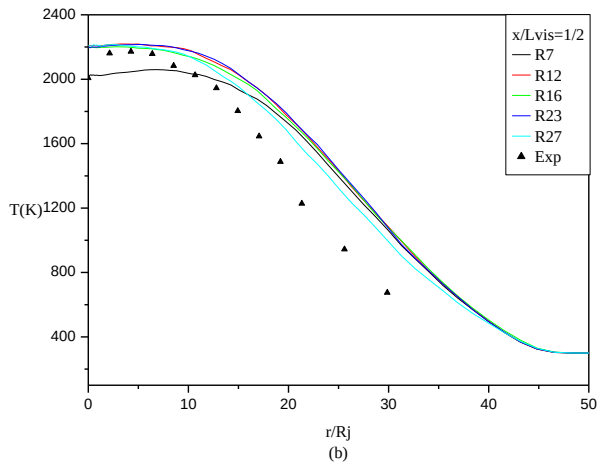

Figure 4. Radial profils of the temperature at x/Lvis= 1/8, 1/2 and 3/4

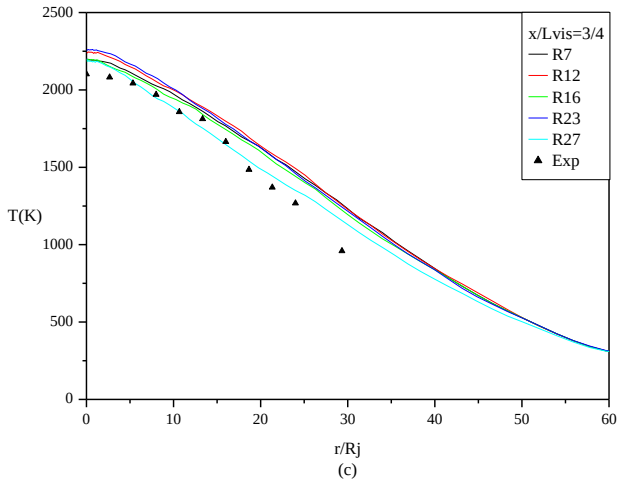

Figure 4. (cont.)

The axial evolution of the mean mixture fraction, as shown in Figure 5, is not influenced by the choice of chemical kinetic mechanisms. A good prediction of experimental data is observed for the five kinetic mechanisms.

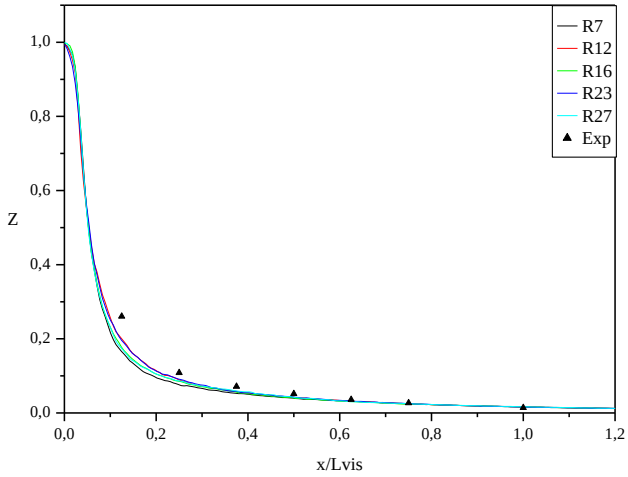

Figure 5. Centerline evolution of the mixture fraction

The radial evolution of the mean mixture fraction at the three axial locations is shown in Figure 6(a), 6(b) and 6(c). It can be seen that the effect of the chemical kinetic mechanisms manifests only in the region very close of the center axis and that this effect becomes negligible, like temperature, for large axial distances. Several factors can interpret the discrepancy between the numerical predictions and the experiment. First, The regions close to the nozzle exit are strongly influenced by the phenomena of chemical kinetics such as the preferential diffusion [18, 19] and the effect of non-equilibrium chemistry [20] which characterizes the hydrogen flames. Also, the inlet boundary conditions have a significant effect on this region [21]. The turbulence model used is another element to consider. Compared to experimental results, the numerical results obtained are generally very satisfactory and in particular in regions with long axial distances (x/L_{vis}=3/4).

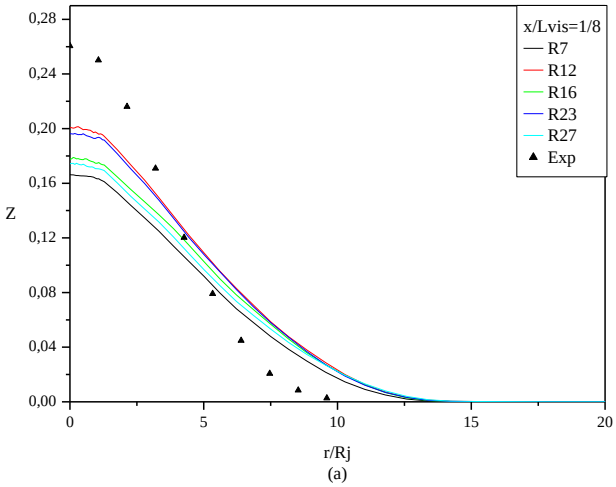

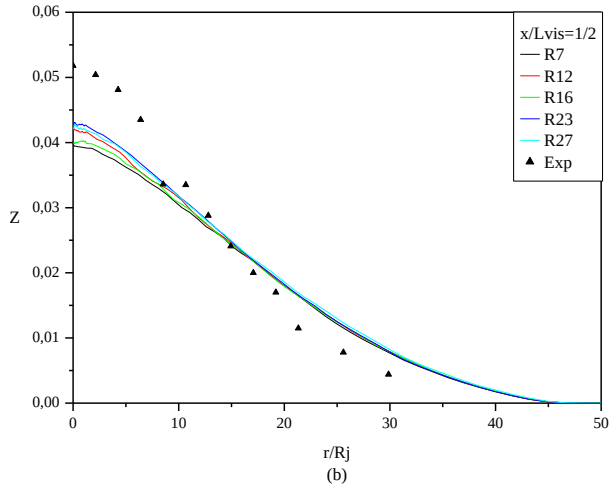

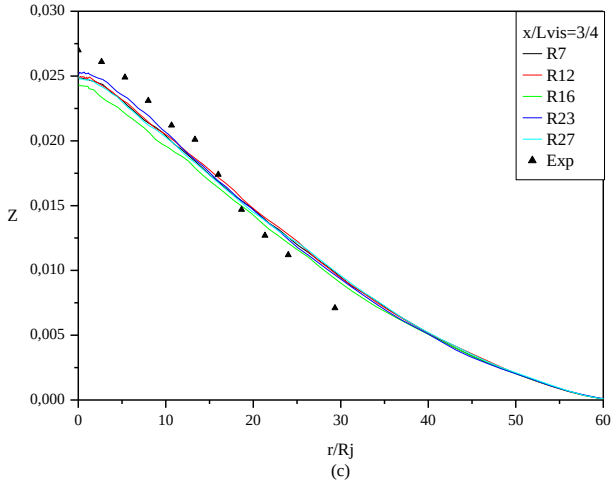

Figure 6. Radial profils of the mixture fraction at x/Lvis= 1/8, 1/2 and 3/4

The axial evolutions of mean profiles of mass fraction of hydrogen, water and oxygen are shown in Figures 7, 8 and 9 respectively. These evolutions are not influenced by the choice of the chemical kinetic mechanisms and the numerical results are in good agreement with experimental data.

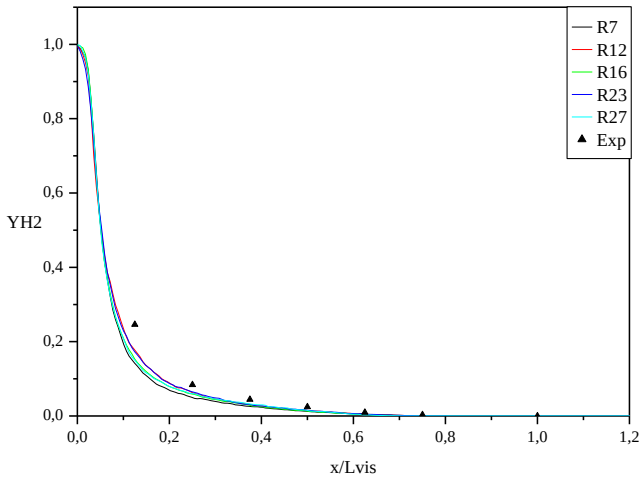

Figure 7. Centerline evolution of the mass fraction of hydrogen

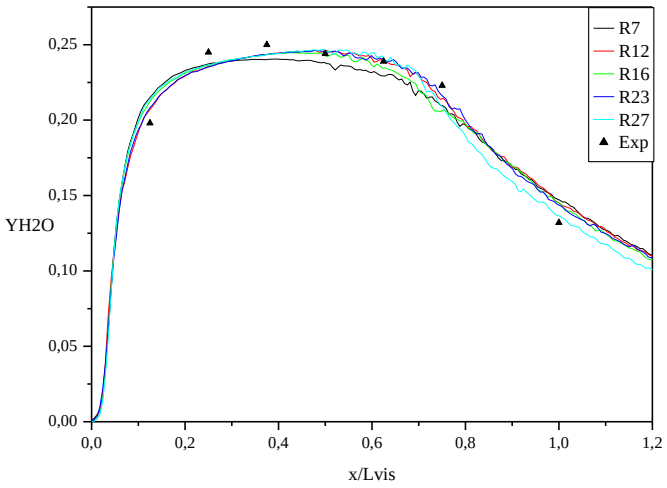

Figure 8. Centerline evolution of the mass fraction of water

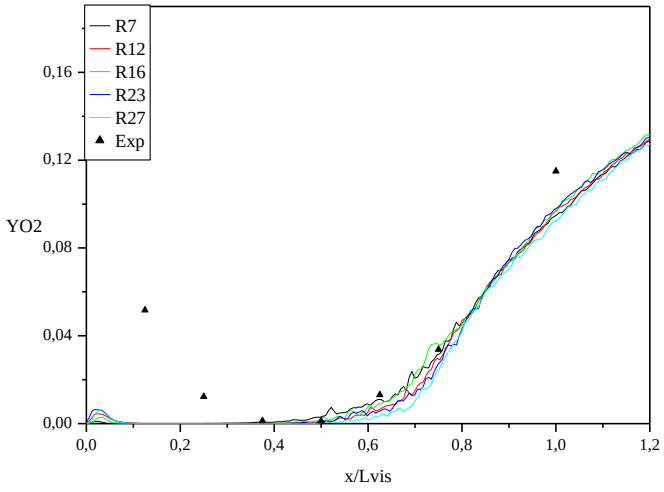

Figure 9. Centerline evolution of the mass fraction of dioxygen

In Figure 10, it can be seen that the axial velocity evolution is insensitive to the choice of kinetic mechanisms. On the other hand, the axial evolution of the turbulent kinetic energy, Figure 11, is slightly affected by this choice. Faster decay of the two chemical kinetic mechanisms R7 and R16 compared to R12, R23 and R27. The effect of chemical kinetics on the dynamic field is through the density.

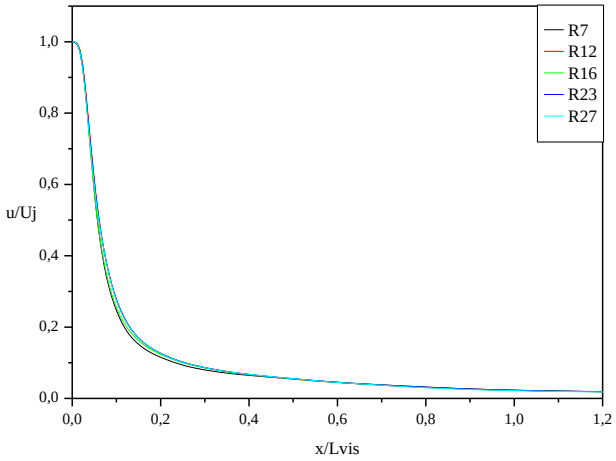

Figure 10. Centerline evolution of the mean velocity

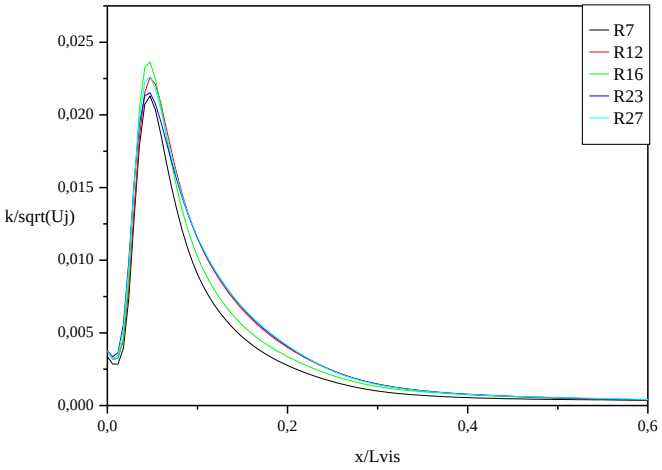

Figure 11. Centerline evolution of turbulent kinetic energy

6.2 Effect of Number of Particles

In this paragraph, the effect of the number of particles on the temperature evolution is analyzed. Two cases were tested: 12 particles (12P) and 20 particles (20P). As shown in the Figures 12 to 17, the number of particles has no influence on the axial evolution of the temperature and this for the two chemical kinetic mechanisms R12 and R27. On the other hand, on the radial evolution, an effect only in the regions very close to the ejection nozzle (x/L_{vis}=1/8) for detailed chemical kinetic mechanism. It can only be said that a detailed kinetic mechanism using an important number of particles can improve the accuracy of the numerical results.

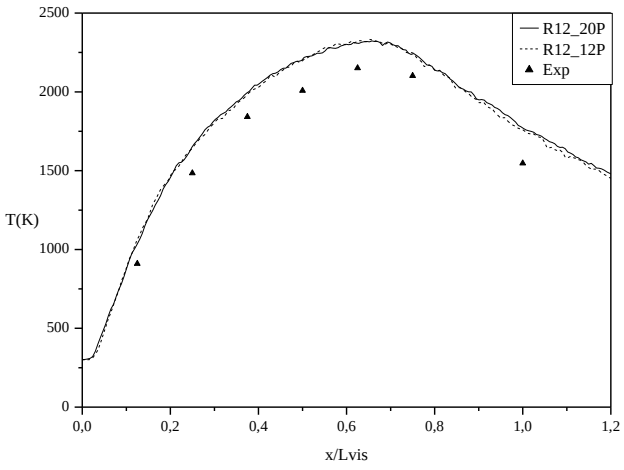

Figure 12. Effect of number particles on the axial evolution of temperature (R12)

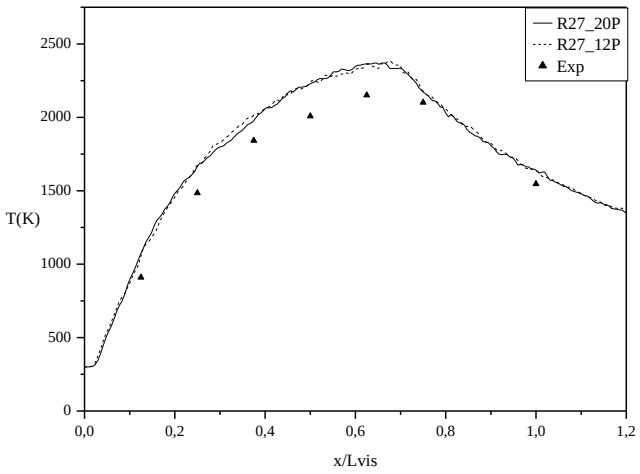

Figure 13. Effect of number particles on the axial evolution of temperature (R27)

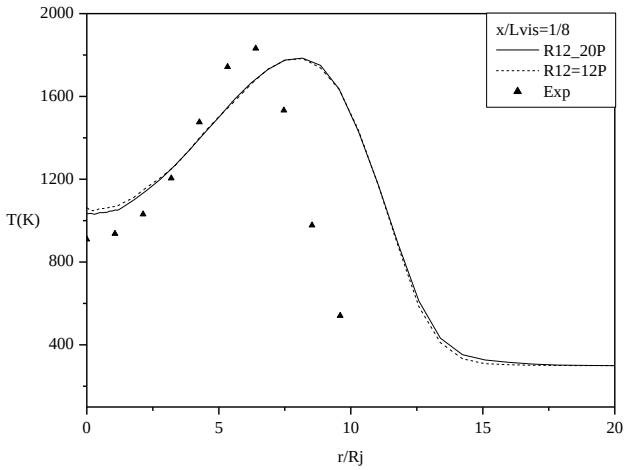

Figure 14. Effect of number particles on the radial evolution of temperature (R12, x/Lvis=1/8)

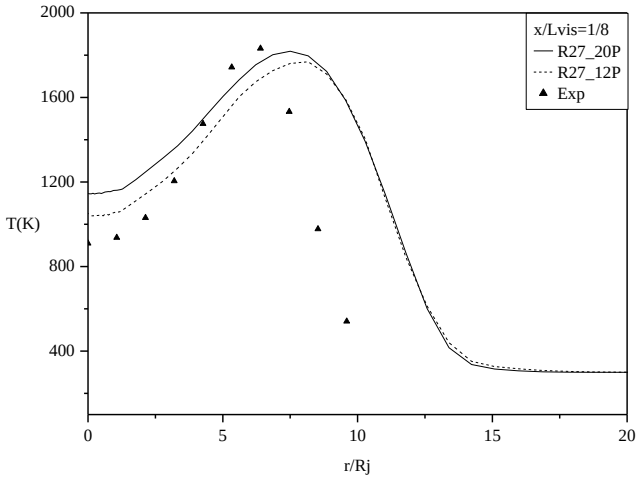

Figure 15. Effect of number particles on the radial evolution of temperature (R27, x/Lvis=1/8)

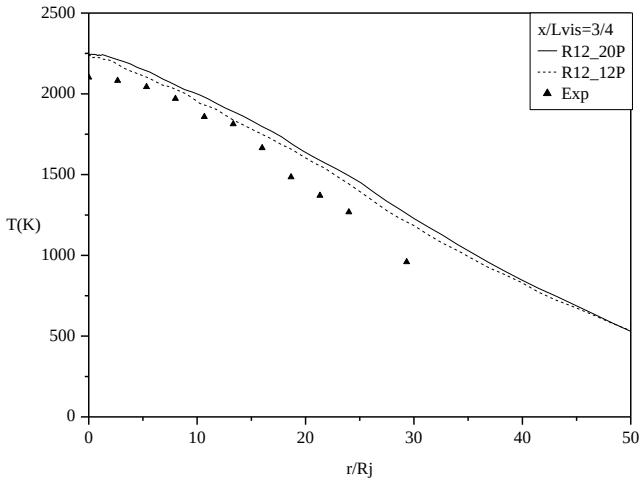

Figure 16. Effect of number particles on the radial evolution of temperature (R12, x/Lvis=3/4)

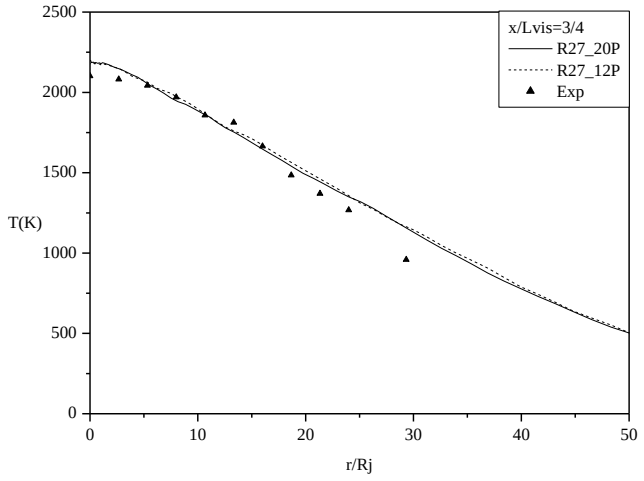

Figure 17. Effect of number particles on the radial evolution of temperature (R27, x/Lvis=3/4)

Table 4 illustrates the effect of particle number on CPU time and storage memory.

Table 4. Effect of number particles

Model	EMST R12	EMSTR27
Particle Number 12		
CPU(s)	87	105
RAM (Mo)	40	51
Iteration count	32	28
Precision %	-10÷10	-3÷3
Particle Number 20		
CPU(s)	145	189
RAM (Mo)	45	53
Iteration count	51	32
Precision %	-5÷5	-1÷1

7.0 CONCLUSION

A hybrid method, Lagrangian PDF/RSM turbulent model, was adopted to study the impact of five different chemical kinetic mechanisms on the scalar and dynamic fields of the turbulent jet diffusion H_2/air flame. The Monte Carlo method, which is highly efficient for high dimensional problems, have been employed to solve the modeled PDF equation. The Favre averaged equations are solved using the finite volume method. The micro-mixing term of PDF equation is modelled by EMST model. The main conclusions of this study are as follows:

1) The scalar field is well influenced by the choice of the chemical kinetic mechanism. This influence is much more evident in the regions close to the nozzle exit.
2) Simple and reduced mechanisms can give satisfactory results in the study of such flames. These kinetic mechanisms are not penalizing in terms of CPU time and storage memory. These kinetic mechanisms can be tested for the prediction of such important phenomena as the ignition and extinction of a flame, the formation of polluting species, etc.
3) The reduced kinetic mechanisms R12 predicts, generally, well the experimental data. This kinetic mechanism can be considered as a compromise between the five kinetic mechanisms. Twelve elementary reactions are therefore sufficient to illustrate the development and behaviour of the scalar field of diffusion hydrogen flames under certain well-defined conditions.
4) Generally, a qualitative and quantitative agreement between experimental results and numerical predictions was found for all the kinetic mechanisms tested.
5) To improve the prediction of turbulent combustion phenomena and to better understand the basic mechanisms that govern them, it is essential to develop new, more, and elaborate models capable of taking into account all the interactions present in a turbulent reactive flow. Also, taking into consideration the influence of phenomena such as thermal radiation and preferential diffusion, which are the main characteristics of hydrogen flames, can greatly improve the quality of numerical prediction. These phenomena are the main characteristics of hydrogen flames.

8.0 NOMENCLATURE

k	Turbulent kinetic energy
P	Instantaneous pressure
R	Perfect gas constant
t	Time
T	Temperature
u_i	Velocity in direction i
$u_i^{''}$	Favre fluctuations of velocity in direction i
Y_α	Species mass fraction of species α
W_α	Atomic weight of species α
ε	Dissipation rate of turbulent energy
Φ	Scalar variable
ρ	Density

9.0 REFERENCES

[1] S. B. Pope, "PDF methods for turbulent reactive flows," *Progress in Energy and Combustion Science*, vol. 11, no. 2, pp. 119-192, 1985.

[2] S. B. Pope, *Turbulent Flows*. Cambridge: Cambridge University Press, 2000.

[3] M. Senouci, A. Bounif, M. Abidat, N. M. Belkaid, C. Mansour, and I. Gokalp, "Transported-PDF (IEM, EMST) micromixing models in a hydrogen-air nonpremixed turbulent flame," *Acta Mechanica*, vol. 224, pp. 3111-3124, 2013.

[4] S. Subramaniam and S. B. Pope, "A mixing model for turbulent reactive flows based on Euclidean minimum spanning trees," *Combustion and Flame*, vol. 115, no. 4, pp. 487-514, 1998.

[5] S. B. Pope, "Computationally efficient implementation of combustion chemistry using in situ adaptive tabulation," *Combustion Theory and Modelling*, vol. 1, no. 1, pp. 41-63, 1997.

[6] R. R. Cao and S. B. Pope, "The influence of chemical mechanisms on PDF calculations of nonpremixed piloted jet flames," *Combustion and Flame*, vol. 143, pp. 450-470, 2005.

[7] J. Li, Z. Zhao, A. Kazakov and F. L. Dryer, "An updated comprehensive kinetic model of hydrogen combustion," *International Journal of Chemical Kinetics*, vol. 36, no. 10, pp. 566 - 575, 2004.

[8] V. P. Zhukov, "Verification, validation, and testing of kinetic mechanisms of hydrogen combustion in fluid-dynamic computations," *ISRN Mechanical Engineering*, vol. 2012, p. 475607, 2012.

[9] D. Fernández-Galisteo, A. L. Sánchez, A. Liñán, and F. A. Williams, "One-step reduced kinetics for lean hydrogen–air deflagration," *Combustion and Flame*, vol. 156, pp. 985-996, 2009.

[10] P. Boivin, "Reduced-kinetic mechanisms for hydrogen and syngas combustion including autoignition," *Doctoral Tesis*, Universidad Carlos III de Madrid, 2011.

[11] X. Zhou, Z. Sun, G. Brenner, and F. Durst, "Combustion modeling of turbulent jet diffusion H_2/air flame with detailed chemistry," *International Journal of Heat and Mass Transfer*, vol. 43, pp. 2075-2088, 2000.

[12] S. Wu, R. Qiu, Y. Jiang, "One-dimensional turbulence simulation of hydrogen-air diffusion flame considering the effects of the differential diffusion," *Journal of Combustion Science and Technology*, vol. 2007, pp. 532-538, 2007.

[13] N. Peters and B. Rogg, "Reduced kinetic mechanisms for applications in combustion systems," *Springer-Verlag*, Germany, 1993.

[14] A. A. Larbi, A. Bounif, M. Senouci, I. Gökalp and M. Bouzit, "RANS modelling of a lifted hydrogen flame using eulerian/ lagrangian approaches with transported PDF method," *Energy, vol. 164, pp. 1242-1256, 2018.*

[15] B. Naud, C. JimeneZ and D. Roekaerts, "A consistent hybrid PDF method: implementation details and application to the simulation of a bluff-body stabilised flame," *Progress in Computational Fluid Dynamics, An International Journal*, vol. 6, no. 1-3, pp. 146-157, 2006.

[16] R. Luppes, "The numerical simulation of turbulent jets and diffusion flames," *Phd Thesis*, Technische Universiteit Eindhoven, 2000.

[17] R. S. Barlow. "Sandia H_2/He flame: Scalar data." *International Workshop on Measurement and Computational of Turbulent Flames*, pp. 1-8, 2003.

[18] W. Meier, A. O. Vyrodov, V. Bergmann, and W. Stricker, "Simultaneous Raman/LIF measurements of major species and NO in turbulent H_2/air diffusion flames," *Applied Physics B*, vol. 63, pp. 79-90, 1996.

[19] J. P. H. Sanders and I. Gokalp, "Nonequilibrium and differential diffusion effects in turbulent hydrogen diffusion flames," *Journal of Thermophysics and Heat Transfer*, vol. 11, pp. 384-390, 1997.

[20] A. Obieglo, J. Gass, and D. Poulikakos, "Comparative study of modeling a hydrogen nonpremixed turbulent flame," *Combustion and Flame*, vol. 122, no. 1, pp. 176-194, 2000.

[21] M. Senouci and A. Bounif, "Simulation numérique d'un jet turbulent axisymétrique à masse volumique variable par le modele au second ordre (RSM)," *Mechanics & Industry*, vol. 12, pp. 315-324, 2011.